2021

Characterization of Oil Droplets in the Upper Cavity of a Rotary Compressor

Puyuan Wu
Purdue University, wu912@purdue.edu

Jun Chen
Purdue University

PaulE. Sojka
Purdue University

Yang Li
Guangdong Meizhi Compressor Co., Ltd.

Hongjun Cao
Guangdong Meizhi Compressor Co., Ltd.

Characterization of Oil Droplets in the Upper Cavity of a Rotary Compressor

Puyuan Wu[1], Jun Chen[1*], Paul E. Sojka[1], Yang Li[2], Hongjun Cao[2]

[1] School of Mechanical Engineering, Purdue University
West Lafayette, IN, USA

[2] Guangdong Meizhi Compressor Co., Ltd.,
Foshan, Guangdong, China

* Corresponding Author: junchen@purdue.edu

ABSTRACT

The lubricant oil is used to lubricate the bearings and seal the clearance between the sliding parts in the rotary compressor equipped in an air conditioning system. However, a portion of the oil is atomized and exhausted with the refrigerant flow, which reduces the system's efficiency and reliability. In this study, a high-resolution shadowgraph system is applied to a modified rotary compressor to visualize the oil droplets in its upper cavity. The oil droplet size distribution is studied statistically at different radial locations and different crankshaft's frequencies. It is observed that more oil droplets with larger D_{10} and D_{32} are generated as the rotating frequency increases. There are fewer droplets moving toward the center of the compressor. More oil droplets in the upper cavity at higher frequency might increase the Oil Discharge Rate (ODR) if these droplets are carried into the downstream discharge tube. On the other hand, larger droplets at a higher frequency may reduce ODR since the appropriate aerodynamic design may retain these droplets in the upper cavity without moving into the discharge tube. The result can assist designers in improving the CFD analysis of compressors and ultimately reducing ODR.

1. INTRODUCTION

Rotary compressors rely on high-speed revolving rolling pistons to compress low-temperature, low-pressure gas-phase refrigerant into superheated vapor that will be discharged into the internal space of the compressor through the discharge port on the cylinder. Lubricant oil is used to lubricate and seal the clearance of sliding parts in the compressor, such as the rolling piston and the cylinder, the vane and the cylinder. Part of the oil in the cylinder will be discharged during the discharge process of the cylinder and atomize into some droplets. Some droplets will follow the gas phase flow, pass through the rotor/stator, enter the compressor's upper cavity, and finally escape from the compressor. The ratio of the escaped oil to the total oil volume is characterized as the Oil Discharge Rate (ODE). The exhausting oil droplets can accumulate in the other parts of the AC system, e.g., the condenser and the evaporator, and significantly lower their heat transfer efficiency and reliability. Thus, lowering ODE is always a key issue for compressor optimization.

Since the atomization of the lubricant oil occurring at the discharge port is complicated and highly coupled to many factors, the oil droplets produced can have different sizes, velocities, and morphological features. Both computational and experimental works are reported about characterizing oil droplets' behavior in the rotary compressor. Wu et al. apply $k-\varepsilon$ model to compute the flow field of refrigerant vapor and use Discrete Phase Method (DPM) method to predict the trajectories of oil particles whose sizes are determined by Rosin-Rammler model (equation 5). Mass flux at the discharge groove and the pressure distribution at the discharge tube are prescribed as inlet and outlet boundary conditions, respectively. In the simulation, oil particles can be bounced off by moving walls or be trapped by stationary walls. Their results show that increasing the upper chamber's height and inserting the discharge tube into the upper chamber can reduce ODR as a result of the improved flow field, which is also verified by experiments (Wu et al., 2015). Noh et al. apply a similar method to analyze the multi-phase flow in a rotary compressor. Their results show that 53% of total oil droplets discharged from the compressor are from the stator core cut and 14% of total oil droplets are from the coil winding area close to the muffler's discharge hole. The percentage will change when the position of the discharge hole on the muffler changes. The number of oil droplets and ODR can be reduced by adding plate type vane in the compressor model used in CFD. They also investigate the oil droplet behavior in the lower cavity, higher cavity, stator core cut, and coil winding area in a rotary compressor experimentally. The mean diameter (D_{10}) is

130 μm in the lower chamber at a rotating frequency of 40 Hz, while over 93.5% of droplets are smaller than 150 μm in the upper chamber. The mean diameter decrease with increased rotating frequency. The speed of droplets in stator core cut and coil winding areas are also evaluated qualitatively.

However, to the best of our knowledge, oil droplets' size distribution in the surrounding area of the discharge tube has not been studied. In this study, the upper cavity refers to the space at the height of the discharge tube's inlet. The modification and optical setup are introduced in the next section, and the statistical analysis of droplets' size is presented in the result section. The conclusion is given in the last section.

2. METHODOLOGY

A twin-cylinder, variable frequency rotary compressor is used as the baseline model. The compressor uses R410a and lubricant of polyol ester, and its discharge pressure (P_D), suction pressure (P_S), and suction temperature (T_S) can be adjusted through a hot-gas bypass test rig. The working conditions are listed in Tab. 1.

Table 1: Experiment Conditions

Crankshaft's Rotating Frequency (Hz)	P_D (MPa)	P_S (MPa)	T_S ($°C$)
30	2.09	1.02	18.1
60	2.54	0.87	12.8
90	3.00	0.71	6.7

Three sapphire optical windows are mounted at the height above the rotor and stator to observe the oil droplets in the compressor's upper cavity, and a lens tube capable of length adjustment is applied to collect data at different radial locations.

A local Cartesian coordinate ($x_3y_3z_3$) is built for the upper cavity measurement, and its origin is at the center of the discharge tube's inlet.

A high-resolution shadowgraph system, as shown in Fig. 1, is set up with a LED light source placed at the 0° window and a 3.2 megapixel CMOS camera placed at the 180° window. The Field of View (FOV) and the Depth of Focus (DOF) of the shadowgraph system are determined by a scale target placed at the focal plane and rotated by 45° with respect to the focal plane. DOF is then $\cos 45°$ times the focused length.

The imaging processing method is used to extract oil droplets recorded by shadowgraph. The routine of the method includes exposure enhancement, de-noise with bilateral filter, calculating the grayscale gradients with Sobel operator and Non-maximum Suppression, Canny operator for edge detection and error checking with Convolutional Neural-Network (CNN).

The uncertainty of the droplet diameter determined from shadowgraph images is estimated to be 1 Pixel (Δl) of the digital imaging sensor. Here we define the characteristic relative uncertainty of droplet diameter as $\Delta l/D_{32}$.

Several characteristic diameters are applied in the current work to study the droplet's size distribution statistically:

Number mean diameter:

$$D_{10} = \frac{1}{N}\sum_{i=0}^{N} D_i. \tag{1}$$

where D_i is the diameter of the ith droplet.

Surface mean diameter (D_{20}):

$$D_{20} = (\frac{1}{N}\sum_{i=0}^{N}(D_i)^2)^{1/2}. \tag{2}$$

Volume mean diameter (D_{30}):

$$D_{30} = (\frac{1}{N}\sum_{i=0}^{N}(D_i)^3)^{1/3}. \tag{3}$$

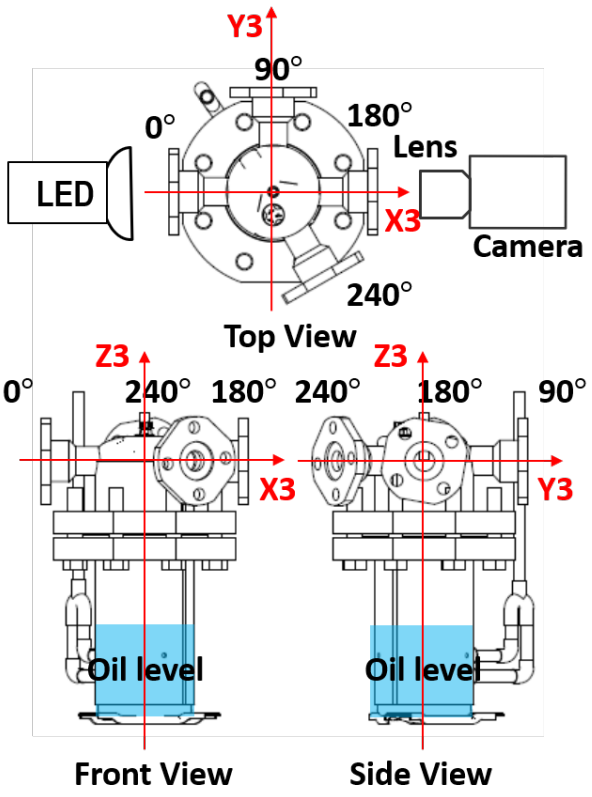

Figure 1: Modification of the discharge tube and optical setup.

Sauter Mean Diameter (SMD or D_{32}):

$$D_{32} = \frac{\frac{1}{N}\sum_{i=0}^{N}(D_i)^3}{\frac{1}{N}\sum_{i=0}^{N}(D_i)^2}. \tag{4}$$

Rosin-Rammler model is used to describe the distribution of droplet sizes:

$$1 - Q = \exp\left(-(\frac{D}{D_{0.632}})^q\right), \tag{5}$$

where Q is the total volume of droplets with a diameter less than D. $D_{0.632}$ denotes the characteristic diameter that 63.2% of the total volume is in droplets with a smaller diameter. q is a constant that describes the uniformity of the droplets' size, and its value increases as the droplets become more uniform.

3. RESULTS AND DISCUSSION

At the height of the discharge tube, the high-resolution droplet's images at different radial positions and frequencies ranging from 30 to 90 Hz are collected, as shown in Fig. 2. The dark region in the background is the discharge tube inserted into the compressor. It can be qualitatively described as that the droplet concentration at each radial location increases as the frequency increases. This is because that more oil is discharged from the cylinder at higher frequencies. Droplets' diameters are extracted and analyzed with the images and are listed in Table. 2-4. D_{10} ranges from 132 to 154 mm, 159 to 188 mm, and 204 to 216 mm at 30, 60, and 90 Hz, respectively. As illustrated in Fig. 3, the characteristic mean diameters have variations within 20% along the radial direction. When comparing droplet size at different frequencies, it is observed that the characteristic mean diameters increase as the frequency increases. The reason is that the refrigerant vapor can carry larger droplets to the height of the discharge tube due to larger velocities. Also, since the gas phase's density increases by 35% due to the higher pressure, while the liquid phase's density only

increases by 4% due to the lower solubility of refrigerant as the frequency increases from 30 to 90 Hz, the ratio of the drag force applied to the droplet to droplet's mass is larger at a higher frequency.

On the other hand, the q values of Rosin-Rammler equation (Equ. 5) at the height of the discharge tube suggest that the droplet's size is close uniform there. It can be explained as that larger droplet existing in the lower area of the compressor is more difficult to be carried to the height of the discharge tube due to the gravity and larger mass, which is also confirmed by the PDF curves (Fig. 4).

Table 2: Characterized Diameter of Oil Droplets at the height of Discharge tube at 30 Hz.

X_3 (mm)	D_{10} (um)	D_{20} (um)	D_{30} (um)	D_{32} (um)	$D_{0.632}$ (um)	q
2.5	138	142	146	155	178	3.89
20.9	143	146	150	157	176	5.15
32.9	154	159	166	179	197	4.36
44	152	155	159	168	190	4.61
61.5	132	137	142	154	184	3.41

Table 3: Characterized Diameter of Oil Droplets at the height of Discharge tube at 60 Hz.

X_3 (mm)	D_{10} (um)	D_{20} (um)	D_{30} (um)	D_{32} (um)	$D_{0.632}$ (um)	q
2.5	184	189	193	203	224	4.96
20.9	188	193	200	213	243	4.30
32.9	180	184	188	197	221	5.24
44	182	186	190	198	220	5.32
61.5	159	163	167	176	200	4.42

Table 4: Characterized Diameter of Oil Droplets at the height of Discharge tube at 90 Hz.

X_3 (mm)	D_{10} (um)	D_{20} (um)	D_{30} (um)	D_{32} (um)	$D_{0.632}$ (um)	q
2.5	216	222	228	241	264	5.50
20.9	209	217	227	247	288	3.50
32.9	204	212	220	238	260	4.67
44	216	223	231	248	268	4.80
61.5	208	213	219	232	254	5.08

4. CONCLUSIONS

In the upper cavity of the rotary compressor, it is observed that, firstly, at 30 to 90 Hz, droplets' size has a close-uniform distribution along the radial direction. The droplets near the wall are slightly smaller than those in the inner region. Secondly, the characteristic mean diameters increase as the frequency increases. Since the flow rate increases at higher frequency, larger flow rates and larger vertical velocity are easier to carry larger droplets. Moreover, as the gas phase density becomes larger at higher frequency, the drag force applied to the droplet is larger. Thirdly, the q values of Rosin-Rammler fitting in all cases are larger than 3.4 and can be greater than 5 in some cases, suggesting that the span of droplet size distribution is small.

REFERENCES

Noh, K., Min, B., Song, S., Yang, J., Choi, G., & Kim, D. (2016, October). Oil droplet behavior with the position of a muffler discharge hole in the shell of a rotary compressor. *Journal of Mechanical Science and Technology*, *30*(10), 4579–4589.

Wu, J., Hu, J., Zhang, J., Sun, M., Wang, G., & Chen, A. (2015). A cfd model for the oil discharge ratio in rotary compressors. *Proceedings of the Institution of Mechanical Engineers, Part A: Journal of Power and Energy*, *229*(2), 151–159.

ACKNOWLEDGMENT

The project is sponsored by Guangdong Meizhi Compressor Co., Ltd..

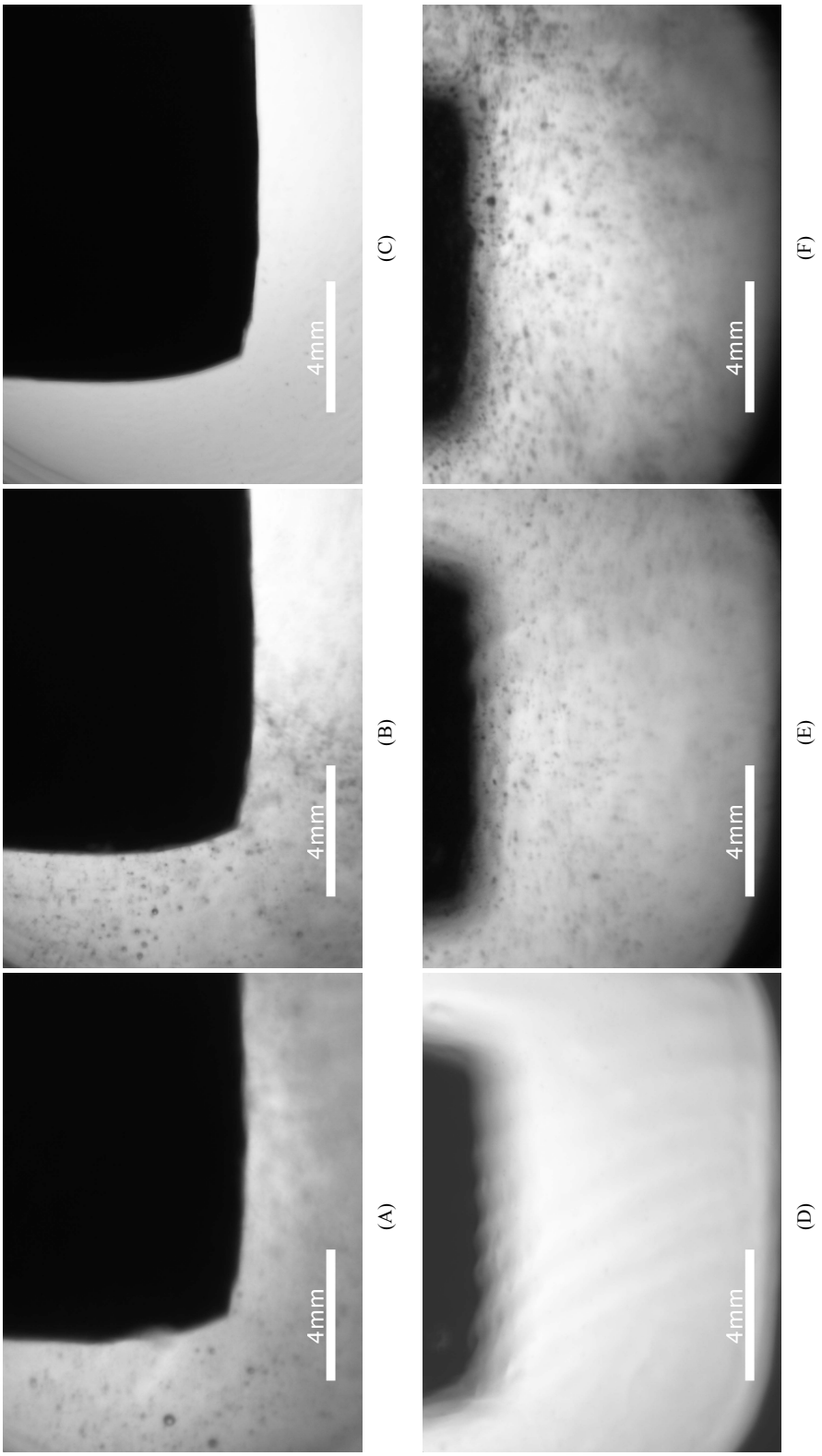
4mm
(A)
4mm
(B)
4mm
(C)
4mm
(D)
4mm
(E)
4mm
(F)

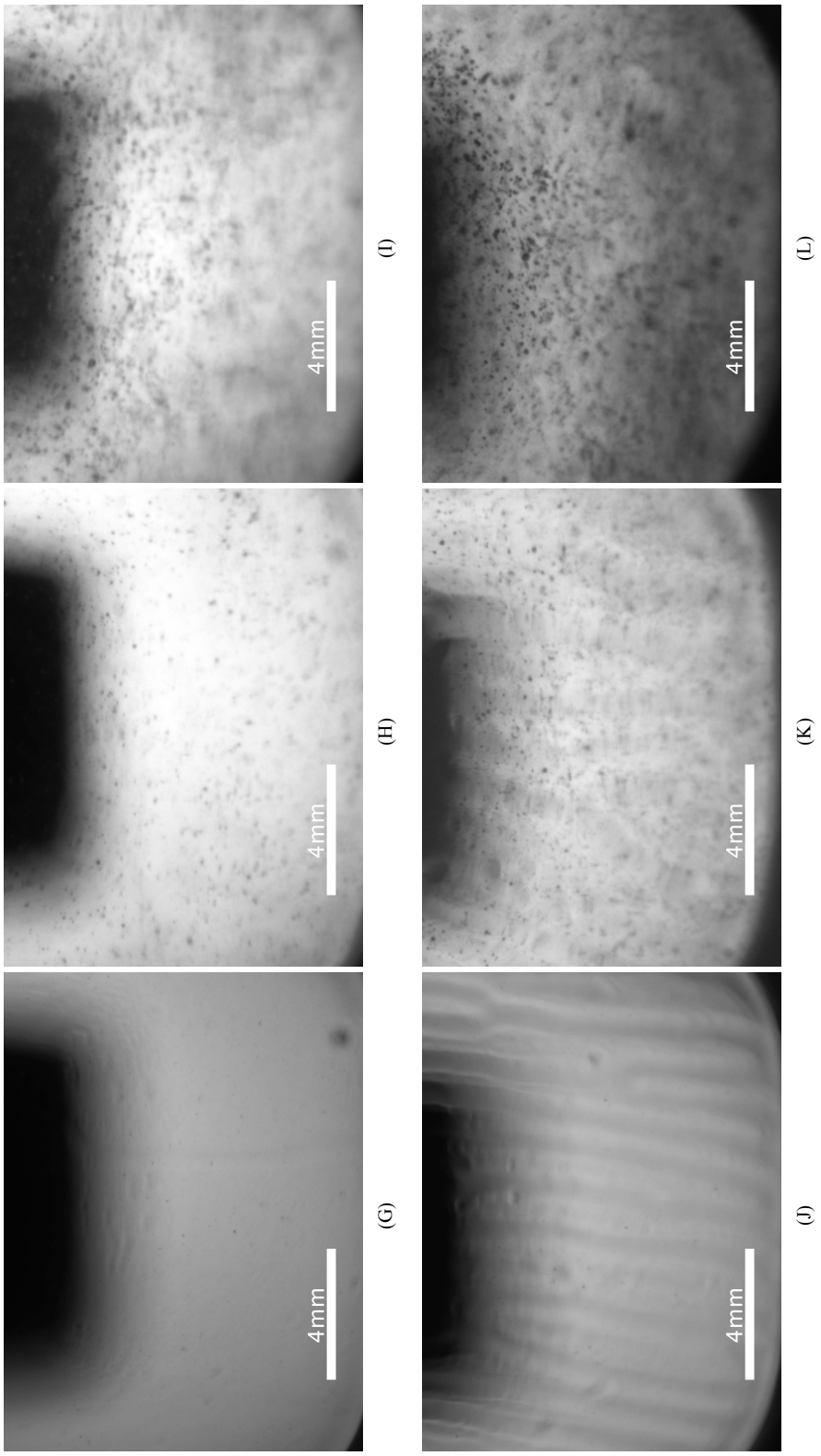
4mm
(I)
4mm
(L)
4mm
(H)
4mm
(K)
4mm
(G)
4mm
(J)

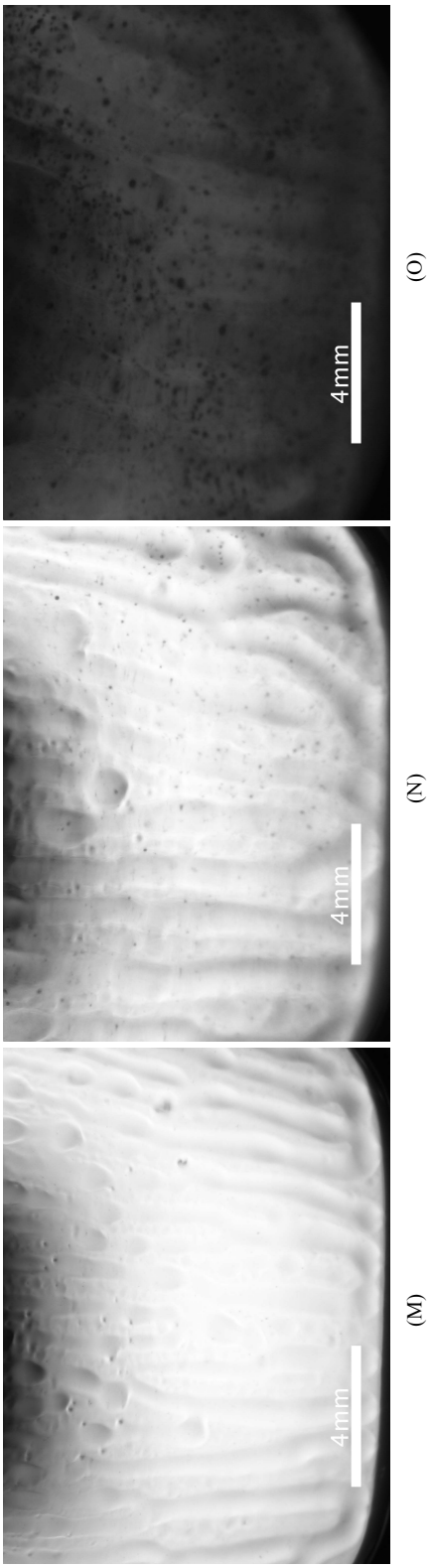

Figure 2: Snapshots of droplets at the height of the discharge tube. (a) 30 Hz, X_3=2.5 mm. (b) 60 Hz, X_3=2.5 mm. (c) 90 Hz, X_3=2.5 mm. (d) 30 Hz, X_3=20.9 mm. (e) 60 Hz, X_3=20.9 mm. (f) 90 Hz, X_3=20.9 mm. (g) 30 Hz, X_3=32.9 mm. (h) 60 Hz, X_3=32.9 mm. (i) 90 Hz, X_3=32.9 mm. (j) 30 Hz, X_3=44 mm. (k) 60 Hz, X_3=44 mm. (l) 90 Hz, X_3=44 mm. (m) 30 Hz, X_3=61.5 mm. (n) 60 Hz, X_3=61.5 mm. (o) 90 Hz, X_3=61.5.5 mm.

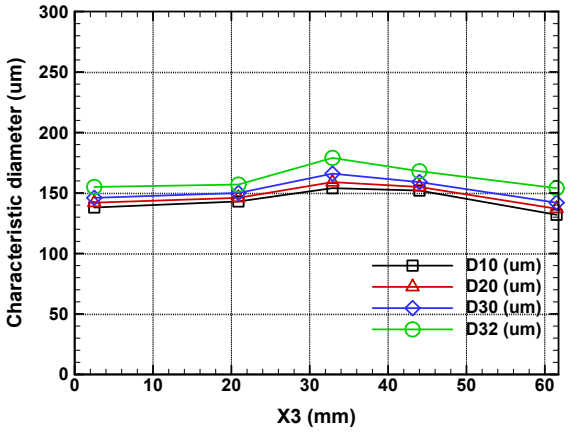

(A)

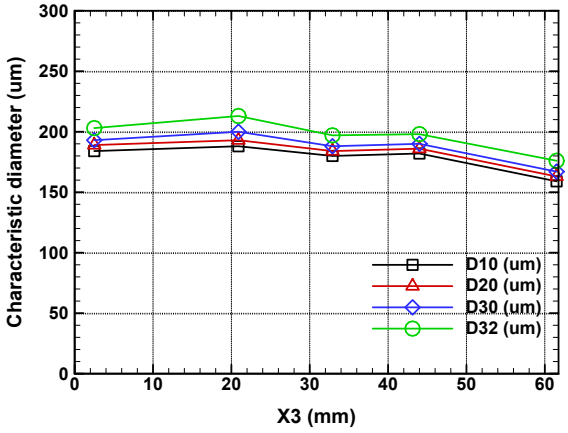

(B)

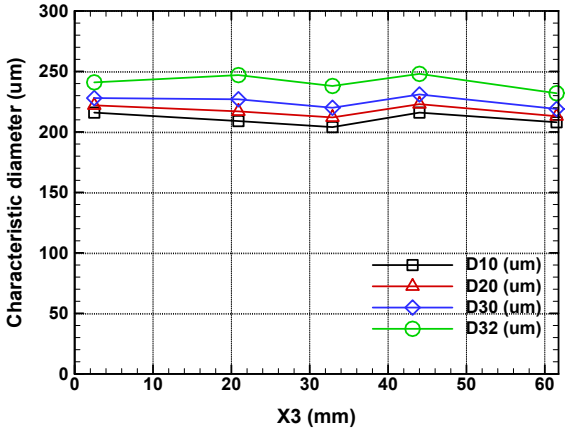

(C)

Figure 3: Characteristic mean diameters' distribution along the radial direction. (a) 30 Hz. (b) 60 Hz. (c) 90 Hz.

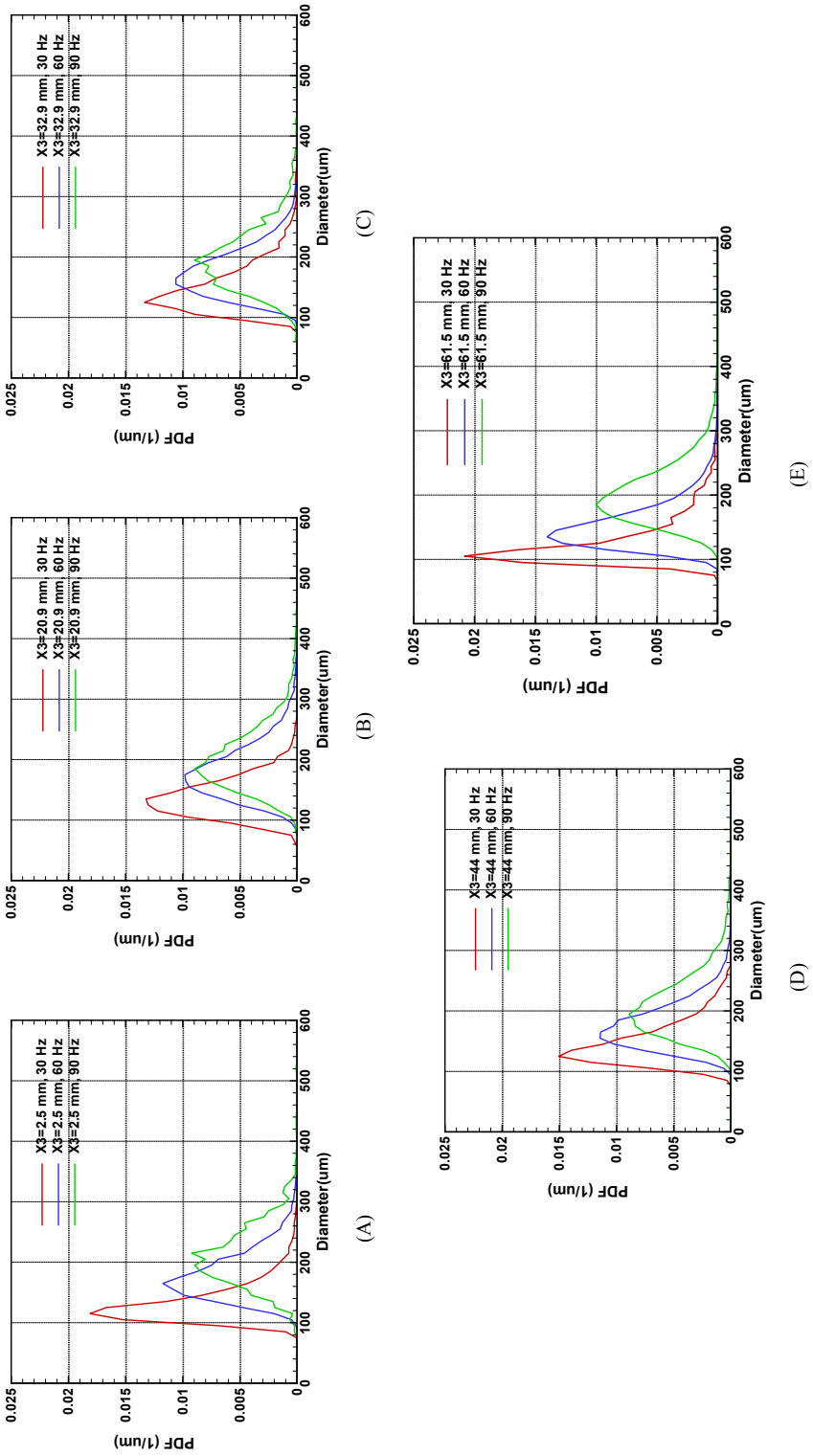

Figure 4: Oil droplets size distribution. (a) X_3=2.5 mm. (b) X_3=20.9 mm. (c) X_3=32.9 mm. (d) X_3=44 mm. (e) X_3=61.5 mm.